

# Capacity scaling in a Non-coherent Wideband Massive SIMO Block Fading Channel

Felipe Gomez-Cuba, *Member, IEEE*, Mainak Chowdhury, *Member, IEEE*, Alexandros Manolakos, Elza Erkip, *Fellow, IEEE*, and Andrea J. Goldsmith, *Fellow, IEEE*

**Abstract**—The scaling of coherent and non-coherent channel capacity is studied in a single-input multiple-output (SIMO) block Rayleigh fading channel as both the bandwidth and the number of receiver antennas go to infinity jointly with the transmit power fixed. The transmitter has no channel state information (CSI), while the receiver may have genie-provided CSI (coherent receiver), or the channel statistics only (non-coherent receiver). Our results show that if the available bandwidth is smaller than a threshold bandwidth which is proportional (up to leading order terms) to the square root of the number of antennas, there is no gap between the coherent capacity and the non-coherent capacity in terms of capacity scaling behavior. On the other hand, when the bandwidth is larger than this threshold, there is a capacity scaling gap. Since achievable rates using pilot symbols for channel estimation are subject to the non-coherent capacity bound, this work reveals that pilot-assisted coherent receivers in systems with a large number of receive antennas are unable to exploit excess spectrum above a given threshold for capacity gain.

**Index Terms**—Massive MIMO, wideband channel, non-coherent Communications, Energy modulation

## I. INTRODUCTION

Spectral efficiency continues to be an important driver for next generation wireless communication systems, including 5G cellular. Hence, communication techniques using large antenna arrays and large bandwidths have attracted significant attention from both industry and academia. Intuitively, increasing the number of antennas and/or the operating bandwidth increases the number of signal dimensions in a communication system, enabling improved performance. However, an accurate knowledge of the wireless channel parameters at the receiver is essential to achieving this performance. Obtaining knowledge of the instantaneous channel state information (CSI) at the receiver becomes increasingly difficult when *either* the number of antennas or the bandwidth is large. This has motivated much work investigating channel capacity under varying degrees of receiver CSI, especially in multi-antenna or wideband systems.

Part of this work was published in the IEEE Information Theory Workshop 2015 [1]. Felipe Gomez-Cuba is with Dipartimento D'ingegneria della Informazione, University of Padova, Italy. Email: gomezcuba@dei.unipd.it Mainak Chowdhury is with ZaiNar, Inc. Email: mainakch@gmail.com Alexandros Manolakos is with Qualcomm Technologies, Inc. - Wireless Research and Development (R&D). Email: amanolak@qti.qualcomm.com Elza Erkip is with NYU Tandon School of Engineering, Brooklyn, NY, USA. Email: elza@nyu.edu. Andrea J. Goldsmith is with the Department of Electrical Engineering, Stanford University, Stanford, CA, US Email: andreag@stanford.edu. This project has received funding from the European Union's Horizon 2020 research and innovation programme under the Marie Skłodowska-Curie grant agreement No 704837, from ONR grant N000141210063, and from the NSF Center for Science of Information (CSol) under grant CCF-0939370.

The impact of receiver CSI on channel capacity may be studied by comparing the capacity of a channel under the assumption that the CSI is perfectly known at the receiver (coherent capacity) with the capacity of a channel where the CSI is unknown (non-coherent capacity). The coherent capacity has been well characterized for many point-to-point channels, including those arising in the context of a multi-antenna or a wideband system [2]. Results for the capacity of the non-coherent channel are more elusive. Existing works on non-coherent channel capacity include [3]–[9], which characterize properties of the capacity, and the capacity-achieving distribution. Some of these works also establish upper and lower capacity bounds for certain channel models.

In addition to capacity expressions and bounds, there has been some recent work which has characterized the asymptotic behavior of the capacity of various noncoherent channels. Two asymptotic regimes that are relevant to our analysis in this manuscript include characterizations of the non-coherent capacity achieving schemes both in asymptotically wideband systems with a fixed number of antennas [10]–[19], and in narrowband systems with an asymptotically large number of antennas [20]–[27].

A major focus in the study of wideband systems with a finite number of antennas is the inherent capacity gap between coherent and non-coherent systems under constraints on the signal “peakiness” [10]–[19]. To narrow or close this gap, it is necessary to use either signals with unbounded peakiness [13]–[15] or to reduce the bandwidth occupancy of the signal by restricting the transmitted signal power to a small subset of the available spectrum [16], [18]. In either case, even though the rate gap is closed with increasing peakiness, the non-coherent receivers have a *second order suboptimality* [12] compared to coherent receivers in terms of capacity growth with increasing bandwidth.

On the other hand, a significant challenge in narrowband systems with large antenna arrays (e.g., in multiuser massive Multiple Input Multiple Output (MIMO) systems) is channel estimation [21], [23]. If the receiver has perfect CSI, the degrees of freedom (DoF) in an i.i.d. Rayleigh channel is the minimum of the number of transmit and receive antennas. This suggests that, if the number of receiver antennas is high and the number of transmit antennas is increased, the DoF, and hence the overall capacity, increases. Without perfect CSI, however, the DoF cannot be increased arbitrarily by having more transmit antennas [26]. In fact in a non-coherent Rayleigh fading channel with the number of transmit antennas greater than the coherence length, it has been shown that the

capacity does not increase at all by adding more transmit antennas [3]. This implies that increasing the number of transmit antennas cannot make the capacity grow indefinitely in the non-coherent channel as in the coherent channel. The capacity can still grow logarithmically with the number of receive antennas in the non-coherent channel [28], [29]. In multiple-user scenarios where the number of users remains constant as the number of antennas scales a similar scaling limitation exists. Motivated by this, in the remainder of the manuscript, we focus on a single user system with a single transmit antenna (point-to-point SIMO channel). With regard to our main result, in the last section of the paper we argue that our main result on capacity scaling for a point-to-point SIMO channel can be extended to MIMO channels and multiuser systems with a finite number of users/transmitters.

In this work, we characterize the capacity scaling of the *block fading wideband massive SIMO channel* and investigate the gap in a scaling law sense between the coherent and non-coherent capacities of this channel as both the bandwidth and the number of receiver antennas jointly scale to infinity. A major difference of our analysis from existing wideband coherent vs. non-coherent capacity comparisons summarized above is that we assume both the number of receive antennas and the bandwidth are very large. Assuming both dimensions scale to infinity reveals the following challenge in applying prior results for scaling across only one of these two dimensions. Prior work on wideband characterizations of non-coherent capacity e.g., [11], [13] with a fixed number of antennas assume a low-SNR regime where the available transmit power is spread across a very wide bandwidth. On the other hand, characterizations of non-coherent narrowband channel capacity with a large number of antennas (e.g., [28], [29]) cannot use low-SNR capacity results since the received SNR does not decrease with the number of antennas. Thus, prior results in only one of these asymptotic regimes are not immediately applicable to the situation where both the bandwidth and the number of antennas scale jointly.

The main contribution of this manuscript is the derivation of capacity scaling for the block fading wideband massive SIMO channel using a non-coherent receiver with knowledge only of the channel statistics. To do this, we first derive a capacity upper bound. Next, we describe an achievable scheme based on the use of energy modulation [28]–[31]. This matches the scaling behavior of the upper bound, thereby establishing the capacity scaling result.

Our analysis reveals that, when the bandwidth is smaller than a threshold bandwidth which is proportional to the square root of the number of antennas, the capacity of the coherent wideband massive SIMO channel displays the same scaling as the capacity of the non-coherent wideband massive SIMO channel. Further capacity gain in a scaling sense cannot be achieved by increasing the bandwidth above this threshold.

An important practical implication of our findings arises for pilot-assisted coherent receivers under our channel model, as compared to coherent receivers with perfect receiver CSI. Since we consider block fading models with any finite block-length, our non-coherent channel capacity scaling analysis is also applicable when a coherent detection technique relies on

pilot-assisted channel estimation rather than perfect CSI. Thus, our analysis suggests that the coherent channel capacity is not necessarily an accurate indicator of rate scaling in practical systems when more spectrum and a larger number of antennas are available, as in the case of 5G. Furthermore, we find numerically that the trends predicted in our capacity scaling law characterization may be applicable outside the asymptotic regimes of large bandwidth and numbers of antennas. In particular, our results indicate that the derived capacity scaling laws are applicable for systems with tens to hundreds of antennas and several tens of MHz of bandwidth which is consistent with the design of some existing wireless systems.

The rest of this paper is structured as follows. Section II describes the general frequency-selective Rayleigh block fading channel model and the different system parameters. Section III describes our main result on capacity scaling. Section IV contains the general analysis strategy and outlines the proof of the converse. Section V describes a scheme based on EM constellations that achieves the capacity scaling. Section VI provides numerical examples, discussion and extensions of the main results in the paper. Finally Section VII concludes the paper.

#### A. Notation

We use uppercase letters (A, B, C, ...) to refer to random variables, and lowercase letters (a, b, c, ...) to refer to their realization. We use script notation  $\mathcal{A}, \mathcal{B}, \dots$  to refer to sets. We use tensor notation (objects with indices) here to refer to collections of objects. If the index of a tensor object is a set, that refers to the collection of all objects with the corresponding indices belonging to the set. For example  $X_{\mathcal{A}}$  represents a one dimensional vector with coefficients  $\{X_a, \forall a \in \mathcal{A}\}$ ,  $x_{\mathcal{A}, \mathcal{B}}$  denotes a two dimensional matrix, and so on.

We use  $f(N) = \Theta(g(N))$  to denote that there exist constants  $c_1, c_2, N_0 > 0$  such that for all  $N > N_0$ ,  $c_1 < \frac{f(N)}{g(N)} < c_2$ , and  $f(N) = o(g(N))$  to denote that  $\lim_{N \rightarrow \infty} \frac{f(N)}{g(N)} = 0$  [32]. We use  $f(N) \lesssim g(N)$  to denote  $f(N) \leq g(N) + o(g(N))$ . We use  $f(N) \doteq g(N)$  to denote  $\lim_{N \rightarrow \infty} f(N) - g(N) = 0$ .

## II. SYSTEM MODEL AND ASSUMPTIONS

We consider a single-antenna transmitter and  $N$  antennas at the receiver. We assume an independent identically distributed (i.i.d.) block fading wideband channel model, such that the bandwidth is divided into a number of independent frequency-flat subchannels. Such a channel may arise, for example, in a rich scattering environment with a high delay spread. We assume that the delay spread is constant

We assume further that the subchannel gains experience Rayleigh fading that is i.i.d. across subchannels and receiver antennas. The validity of this assumption depends on wireless propagation in the bands of operation and on the number of receiver antennas. In sub-6 GHz bands with a rich scattering environment, this assumption is typically more accurate than in mmWave bands (e.g., 28 GHz, 38 GHz, 60 GHz) where the propagation is more specular. And less scattering leads

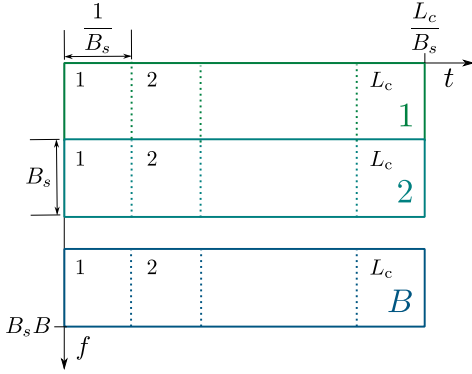


Fig. 1: Block-fading frequency-selective channel consisting in  $B$  independent subchannels of bandwidth  $B_s$  each, where each subchannel experiences flat i.i.d. Rayleigh block-fading with block length  $L_c$ .

to more correlation across fading realizations. Our analysis does not apply in channels when the i.i.d. assumption is not valid. Some existing work on wideband sparse channels have reported an “overspreading” phenomenon similar to ours. We discuss this related work and possible extensions in Section VI-E.

We take the subchannel bandwidth to be the coherence bandwidth  $B_c$  which is assumed fixed in this manuscript. We also assume that the coherence time is fixed, equal to  $L_c$  symbols and that each subchannel experiences narrowband block fading [2]. The number of subchannels is  $B$ , thus the total bandwidth is  $BB_s$ .

The channel can be represented on the resource grid depicted in Figure 1 where we denote the transmitted symbol indices by  $\ell \in \{0, \dots, L_c - 1\} \triangleq \mathcal{L}$ , the receive antennas by  $r \in \{0, \dots, N - 1\} \triangleq \mathcal{N}$ , and the subchannels by  $m \in \{0, \dots, B - 1\} \triangleq \mathcal{B}$ . For each triplet  $(r, m, \ell) \in \mathcal{N} \times \mathcal{B} \times \mathcal{L}$  the channel output  $Y_{r,m,\ell}$  is given by

$$Y_{r,m,\ell} = H_{r,m} X_{m,\ell} + Z_{r,m,\ell}. \quad (1)$$

where  $Z_{r,m,\ell} \sim \mathcal{CN}(0, 1)$  is Additive White Gaussian Noise (AWGN).  $H_{r,m} \sim \mathcal{CN}(0, 1)$  is the channel gain, which is i.i.d. for each  $r$  and  $m$  but remains constant over all  $\ell \in \mathcal{L}$ , and  $X_{m,\ell}$  is the channel input, where the set of transmitted symbols  $X_{\mathcal{B},\mathcal{L}}$  are subject to the power constraint

$$\mathbb{E} \left[ \frac{1}{BL_c} \sum_{\ell \in \mathcal{L}} \sum_{m \in \mathcal{B}} |X_{m,\ell}|^2 \right] \leq P, \quad (2)$$

where  $P$  is the average power available to the single-antenna transmitter. This is the block Rayleigh fading model with coherence block length  $L_c$ . In this paper we assume  $L_c$  and  $P$  are constants; furthermore  $L_c = \Theta(1)$  and  $P = \Theta(1)$  will be used interchangeably since we study the scaling behavior.

In our analysis we compare the ergodic capacity [2] of coherent and non-coherent channels as defined below. Ergodic capacity is a more appropriate performance indicator than capacity with outage in modern wireless technologies with turbo coding and hybrid automated repeat request [33]. Furthermore, we assume no transmitter CSI for both the coherent and the

non-coherent systems.

**Definition 1.** We define the **coherent** ergodic capacity of the block fading Rayleigh channel as a function of  $N$  and  $B$  as

$$C_c(N, B) = \sup_{p(X_{\mathcal{B},\mathcal{L}})} \mathbb{E}_{H_{\mathcal{N},\mathcal{B}}} [\mathbb{I}(X_{\mathcal{B},\mathcal{L}}; Y_{\mathcal{N},\mathcal{B},\mathcal{L}} | H_{\mathcal{N},\mathcal{B}})] \quad (3)$$

**Definition 2.** We define the **non-coherent** ergodic capacity of the block fading Rayleigh channel as a function of  $N$  and  $B$  as

$$C_n(N, B) = \sup_{p(X_{\mathcal{B},\mathcal{L}})} \mathbb{E}_{H_{\mathcal{N},\mathcal{B}}} [\mathbb{I}(X_{\mathcal{B},\mathcal{L}}; Y_{\mathcal{N},\mathcal{B},\mathcal{L}})] \quad (4)$$

Here, note that  $C_c(N, B)$  and  $C_n(N, B)$  are specified in units of bits per fading block. The coherent capacity can be put in bits per channel use as  $\frac{B_s}{L_c} C_c(N, B)$  where  $\frac{B_s}{L_c}$  is a constant that does not affect scaling results, and likewise for the non-coherent capacity. Note also that the supremum is outside the expectation operator and  $p(X_{\mathcal{B},\mathcal{L}})$  does not depend on the channel, as there is no feedback nor CSI at the transmitter.

In our analysis, we will study the scaling of  $C_c(N, B)$  and  $C_n(N, B)$  asymptotically as  $B, N$  both go to infinity according to the following relation:

$$\epsilon = \lim_{B, N \rightarrow \infty} \frac{\log(B)}{\log(N)}, \quad (5)$$

for a non-negative constant  $\epsilon$ . This may equivalently be expressed as  $B = \Theta(N^\epsilon)$ .

### III. MAIN RESULT

#### A. Coherent capacity scaling

We begin by formalizing the scaling of the capacity of the coherent channel  $C_c(B, N)$  for large  $N$ . Since optimal inputs and receiver combining are well known for the SIMO channel with perfect CSI, the scaling result follows from simple observations on known expressions.

**Lemma 1.** For  $\epsilon < 1$ , the capacity of a coherent block Rayleigh fading i.i.d. wideband SIMO channel with  $N$  receive antennas and bandwidth  $B = \Theta(N^\epsilon)$ , where  $H_{\mathcal{N},\mathcal{B}}$  is known perfectly at the receiver, and the transmitter has no CSI nor feedback, scales as

$$C_c(B, N) = \Theta(N^\epsilon \log(N)). \quad (6)$$

For  $\epsilon \geq 1$  it scales as

$$C_c(B, N) = \Theta(N). \quad (7)$$

*Proof.* The SIMO channel capacity with perfect CSI at the receiver is well known. We consider a SIMO model where for each pair  $(m, \ell) \in \mathcal{B} \times \mathcal{L}$  the subchannel  $H_{\mathcal{N},m}$  is an independent vector. Since there is no feedback or CSI at the transmitter, the ergodic capacity is achieved using Gaussian inputs with equal power in all subchannels [2]. Since there is

only one transmit antenna, maximal ratio combining can be used at the receiver and the capacity is

$$C_c(N, B) = \mathbb{E}_{H_{N,m}} \left[ BB_s \log \left( 1 + \frac{P(\sum_{r=0}^{N-1} |H_{r,m}|^2)}{B} \right) \right] \text{ bit/s.} \quad (8)$$

The expectation is taken over the randomness in the sub-channel coefficients.  $\sum_{r=0}^{N-1} |H_{r,m}|^2$  is chi-square distributed with  $2N$  degrees of freedom and in the limit  $N \rightarrow \infty$  the term  $\frac{P(\sum_{r=0}^{N-1} |H_{r,m}|^2)}{B} \rightarrow \frac{NP}{B}$  concentrates sharply around a quantity proportional to  $N^{1-\epsilon}$ , since  $P$  is constant. Thus, with  $\epsilon < 1$ , the ergodic capacity scales as  $\Theta(B \log(N))$ . For  $\epsilon = 1$ , the SNR per subchannel does not increase, hence the ergodic capacity scales as  $\Theta(B) = \Theta(N)$ . Finally, for  $\epsilon > 1$  the capacity expression is the same but the effective SNR per subchannel decreases as  $N$  increases. Using the approximation  $\log(1+x) \simeq x$  for  $x \ll 1$  the ergodic capacity is proportional to  $\frac{N^{1+\epsilon}}{N^\epsilon}$  for sufficiently large  $N$ , which reduces to  $\Theta(N)$ .  $\square$

### B. Non-coherent capacity scaling

A closed form expression for the capacity of the general multi-antenna non-coherent channel is not available. Instead, we characterize the scaling behavior of an upper bound to the capacity and show that a scheme with the same rate scaling exponent is achievable. The upper bound and achievable scheme coincide in a scaling law sense but the corresponding rates may differ by constant or lower order terms.

**Theorem 1.** *The capacity scaling for the non-coherent block fading i.i.d. Rayleigh wideband SIMO channels with  $N$  receive antennas and bandwidth  $B = N^\epsilon$ , with a finite coherence time  $L_c$ , satisfies*

$$\Theta(N^{\min(\epsilon, \frac{1}{2}) - \alpha}) \leq C_n(B, N) \leq \Theta(N^{\min(\epsilon, \frac{1}{2}) + \alpha}) \quad (9)$$

for all  $\alpha > 0$ .

*Proof.* The proof is trivial for  $\epsilon < \frac{1}{2}$ , for which we use the coherent capacity bound, i.e.,

$$C_n(B, N) \leq C_c(B, N).$$

Therefore with  $\epsilon < \frac{1}{2}$  the upper bound is  $C_n(B, N) \leq \Theta(N^\epsilon)$ . In addition, the EM scheme discussed in Section V achieves a rate  $\Theta(N^\epsilon)$  with a vanishing error probability if and only if  $\epsilon < \frac{1}{2}$ . In addition, for the case  $\epsilon > \frac{1}{2}$  it is trivial to construct an achievable scheme by using a subset of the channels, i.e., selecting  $B' = \sqrt{N} < B$  subchannels to transmit using the same EM scheme described in Section V. Hence, the remainder of the proof consists in showing that when  $\epsilon > \frac{1}{2}$  a rate scaling  $\Theta(N^\epsilon)$  is not achievable when the channel realization is not known at the receiver. In a prior work [1],

we derived a bound on the same exponent for the achievable rate with inputs subject to a PAPR (peak to average power ratio) constraint with the fading blocklength  $L_c = 1$ . In the current work, we do not make any assumptions on the PAPR or  $L_c$ , except for the latter staying constant.

We establish a capacity upper bound for  $\epsilon > \frac{1}{2}$  in Section IV. This reveals that any capacity optimal scheme cannot use bandwidth more than  $\Theta(N^{\frac{1}{2}})$ . We then show in Section V, an achievability result using energy modulation which matches the capacity scaling in the sense of the theorem above. This establishes the theorem.  $\square$

Comparing Lemma 1 and Theorem 1, we observe that the capacities of coherent and non-coherent channels scale the same way when the bandwidth scales slower than a certain threshold ( $\Theta(N^{1/2})$ ), whereas beyond that threshold, additional bandwidth does not help increase the non-coherent capacity scaling.

Furthermore, we have the following corollary:

**Corollary 1.** *The capacity scaling of coherent and non-coherent receivers is the same in a wideband massive SIMO system if the bandwidth is lower than a threshold bandwidth proportional to the square root of the number of antennas.*

*Proof.* This follows directly from Lemma 1 and Theorem 1.  $\square$

**Remark 1.** *There is a rate scaling gap between genie-aided coherent receivers and pilot-assisted coherent receivers when the bandwidth scales faster than  $\Theta(N^{1/2})$  in a wideband block Rayleigh fading SIMO channel.*

This remark follows from that fact that coherent receivers considered in this manuscript use genie-aided perfect noiseless CSI, which involves knowing  $H_{N,B}$  perfectly. CSI obtained in any practical wireless system is not perfect, it is always acquired through the use of pilot symbols in a noisy channel. Thus pilot-assisted coherent receivers which perform channel estimation and symbol demodulation separately are also subject to the non-coherent capacity limit derived in this manuscript.

These implications will be illustrated through simulation results in Section VI-C.

## IV. PROOF OF THE CONVERSE

In this section, we derive an upper bound on the capacity of the SIMO system per subchannel (10). We then exploit the fact that the wideband SIMO channel consists of multiple parallel subchannels which are statistically identical to derive a final upper bound on the capacity.

$$\begin{aligned} C_n(B, N) &= \max_{p(X_{B,\mathcal{L}}): \mathbb{E}[\frac{1}{BL_c} \sum_{\ell \in \mathcal{L}} \sum_{m \in \mathcal{B}} |X_{m,\ell}|^2] \leq P} \mathbb{E}_{H_{N,B}} [\mathbb{I}(X_{B,\mathcal{L}}; Y_{N,B,\mathcal{L}})] \\ &= \max_{\rho_{\mathcal{B}}: \sum_{m \in \mathcal{B}} \rho_m \leq P} \sum_{m \in \mathcal{B}} \max_{p(X_{m,\mathcal{L}}): \mathbb{E}[\frac{1}{L_c} \sum_{\ell \in \mathcal{L}} |X_{m,\ell}|^2] \leq \rho_m} \mathbb{E}_{H_{N,m}} [\mathbb{I}(X_{m,\mathcal{L}}; Y_{N,m,\mathcal{L}})] \end{aligned} \quad (10)$$

### A. Determining the number of active subchannels

Due to the fact that the channel coefficients  $H_{r,m}$  in (1) are independent and the transmitter has no CSI or feedback, the mutual information maximization problem in (10) can be expressed as the separate maximization problems over a collection of parallel subchannels coupled together only by the average input power constraint.

We observe that when  $\rho_m$  is fixed, the maximization problems over the subchannels are decoupled. We can define the maximum mutual information achievable on subchannel  $m$  as a function of the subchannel transmit power  $\rho_m$  as follows:

$$f_{C,m}(\rho_m) \triangleq \max_{\substack{p(X_{m,\mathcal{L}}): \\ \mathbb{E}\left[\frac{\sum_{\ell \in \mathcal{L}} |X_{m,\ell}|^2}{L_c}\right] \leq \rho_m}} \mathbb{E}_{H_{N,m}} [\mathbb{I}(X_{m,\mathcal{L}}; Y_{N,m,\mathcal{L}})]. \quad (11)$$

Since the  $H_{r,m}$  in (1) are i.i.d., the function  $f_{C,m}(\cdot)$  is the same for all subchannels. We denote this by dropping the index  $m$ . This allows us to rewrite the capacity of the wideband channel as the following sum of identical subchannel capacity functions.

$$C_n(B, N) = \max_{\rho_m: \sum_{m \in \mathcal{B}} \rho_m \leq P} \sum_{m \in \mathcal{B}} f_C(\rho_m) \quad (12)$$

We observe that  $f_C(\rho_m)$  is a non-decreasing function of  $\rho_m$ . By the symmetry of the problem and the KKT conditions, the optimal capacity achieving solution consists of selecting a certain number of subchannels and dividing the total transmit power equally across them.

This means that the non-coherent capacity of the wideband channel can be written as

$$C_n(B, N) = \max_{M \in \{1 \dots B\}} M f_C\left(\frac{P}{M}\right) \quad (13)$$

where, to fully characterize capacity, we would have to address two optimizations: first, find the optimal per-subchannel input distribution in (11) when  $\rho_m = \frac{P}{M}$ ; and second, find the optimal number of subchannels that must be used in order to maximize (13), denoted by  $M^*$ .

### B. Separation of Energy and Shape Distributions

The following lemma is Theorem 2 in [3], particularized from MIMO to SIMO and written using our notation. We will use this lemma to simplify the inner optimization contained in (11).

**Lemma 2. (Theorem 2 of [3])** *The optimal distribution for a frequency-flat Rayleigh block fading  $1 \times N$  SIMO (sub)channel is  $X_{m,\mathcal{L}} = \sqrt{A_m} U_{m,\mathcal{L}}$  where  $A_m$  and  $U_{m,\mathcal{L}}$  are independent,  $A_m$  is a non-negative real number distribution and  $U_{m,\mathcal{L}}$  is an Isotropically Distributed Unitary Vector (IDUV).*

Using this result the input optimization problem in (11) reduces as follows: given  $X_{m,\mathcal{L}} = \sqrt{A_m} U_{m,\mathcal{L}}$  with known optimal  $p(U_{m,\mathcal{L}})$ , we need only to optimize  $\mathbb{I}(\sqrt{A_m} U_{m,\mathcal{L}}; Y_{N,m,\mathcal{L}})$  over  $\{p(A_m) : \mathbb{E}[A_m] = \rho_m\}$ . Still, the amplitude distribution optimization over  $p(A_m)$  contained

in  $f_C(\rho_m)$  to characterize capacity exactly remains elusive. Instead, in Sections IV-C and IV-D we obtain scaling upper bounds on  $f_C(\frac{P}{M})$  as a function of  $M$  and based on these results we identify a limit to the scaling of the optimal number of subchannels  $M^*$  and obtain an upper bound on capacity scaling, i.e. on the scaling of  $M^* f_C(\frac{P}{M^*})$ . In addition, we present an EM scheme in Section V that achieves the capacity scaling upper bounds in all regimes and thus shows our result fully characterizes the capacity scaling.

This generalizes our prior result in [1] where we had employed a different proof that required two assumptions: that the fading blocklength was one ( $L_c = 1$ ) and that the input distribution  $p(X_{m,\mathcal{L}})$  was subject to a peak power constraint. For ease of presentation, we introduce our extension by first removing one constraint, the peak power constraint, while keeping the other,  $L_c = 1$  in Section IV-C, and next we generalize the proof to  $L_c > 1$  in Section IV-D.

### C. Scaling upper bound for $C_n(B, N)$ with $L_c = 1$ , $\epsilon > \frac{1}{2}$

Taking Lemma 2 (i.e. Theorem 2 of [3]),  $L_c = 1$  implies that the isotropic vector  $U_{m,\mathcal{L}}$  becomes a random phase that cannot be recovered by the receiver, and the rate depends completely on the information carried by the distribution of the input energy, i.e.,  $p(A_m)$  with  $A_m = |X_{m,0}|^2$ . In this subsection, we assume that the transmit power is spread equally across  $M$  “active” subchannels and investigate if the total capacity, i.e.,  $M f_C(P/M)$ , can exceed  $\Theta(N^{\frac{1}{2}+\epsilon})$  for any positive  $\epsilon$ . We focus on the case when the bandwidth scales like  $M = \Theta(N^{\frac{1}{2}+\alpha})$  for  $\alpha > 0$ , since when the bandwidth scales like  $\Theta(N^{\frac{1}{2}-\alpha})$  for any positive  $\alpha$ , our achievable scheme achieves the scaling behavior of the coherent channel capacity scaling. With  $M = \Theta(N^{\frac{1}{2}+\alpha})$  we have the following upper bound for the capacity function in each active subchannel.

**Lemma 3.** *When  $M = \Theta(N^{\frac{1}{2}+\alpha})$  with  $\alpha > 0$ ,  $\rho_m = \frac{P}{M}$  and  $L_c = 1$ , the subchannel capacity function (11) satisfies*

$$f_C(P/M) \leq \Theta\left(\frac{1}{N^{2\alpha}}\right). \quad (14)$$

*Proof.* Appendix A provides the proof for this. The proof relies on the observation that when two values of input energies  $a_m, a'_m \sim A_m$  are close to each other, the output distributions  $p(Y_{N,m,\mathcal{L}}|a_m)$  and  $p(Y_{N,m,\mathcal{L}}|a'_m)$  are indistinguishable in a sense made precise in Appendix A. Moreover, the input energies cannot be too far away from zero without violating the average energy constraint.  $\square$

**Remark 2.** *Lemma 3 implies that when there are  $M = \Theta(N^{\frac{1}{2}+\alpha})$  “active” subchannels, the total mutual information in the wideband channel is given by*

$$M f_C(P/M) \leq \Theta(N^{\frac{1}{2}-\alpha}). \quad (15)$$

*Therefore for any  $\alpha > 0$  we have  $M f_C(P/M) = \Theta(N^{\frac{1}{2}-\alpha}) \leq \sqrt{N} f(P/\sqrt{N}) = \Theta(N^{\frac{1}{2}})$ . Therefore the optimal allocation  $M^*$  that maximizes (13) satisfies  $M^* \leq \Theta(N^{\frac{1}{2}})$ . Since  $f_C(P/M^*)$  decreases with  $M^*$ ,  $M^* f_C(P/M^*) \leq \Theta(M^*) \leq$*

$\Theta(N^{\frac{1}{2}})$ , and thus the converse of Theorem 1 with  $\epsilon > \frac{1}{2}$  is proven for  $L_c = 1$

#### D. Upper bound on non-coherent capacity scaling, $L_c > 1$

For the case  $L_c > 1$ , the Marzetta-Hochwald optimal input result in Lemma 2 [3] gives an input with the isotropic vector  $U_{m,\mathcal{L}}$  with more than one component. In the case  $L_c = 1$  no information about  $U_{m,\mathcal{L}}$  could be recovered from the channel output, but for  $L_c > 1$  the channel output may give information about  $U_{m,\mathcal{L}}$  in the sense that some phase-differences and amplitude-differences between  $U_{m,\ell}$  and  $U_{m,\ell+1}$  might be recoverable. Therefore, to construct the extension of Lemma 3, the main difference from the proof when  $L_c = 1$  is we must show that, when the sequence length  $L_c$  is a constant that does not scale with  $N$ , instead of “all the rate”, now “most of the rate” depends on the information carried by the distribution of energy of the input. The input energy density is now defined as  $p(A_m)$  where the energy satisfies  $A_m = \sum_{\ell=0}^{L_c-1} |X_{m,\ell}|^2$ . The exact sense in which “most of the rate” is interpreted is made clear in the proof.

We state the new lemma for the mutual information per subchannel as follows

**Lemma 4.** *When  $M = \Theta(N^{\frac{1}{2}+\alpha})$ , with  $\alpha > 0$ ,  $\rho_m = \frac{P}{M}$  and  $L_c \geq 1$  remains constant as  $N$  grows, the subchannel capacity function (11) satisfies*

$$f_C(P/M) \leq \Theta\left(\frac{1}{N^{2\alpha}}\right). \quad (16)$$

*Proof.* Details are presented in Appendix B.  $\square$

**Remark 3.** *Although the proof requires additional steps, the scaling bound in Lemma 4 takes the same value as in Lemma 3. Therefore Remark 2 applies also to the general case  $L_c \geq 1$ .*

## V. ACHIEVABILITY USING ENERGY MODULATION

We consider the wideband counterpart of the EM scheme initially described in [28], [29] for a narrowband non-coherent massive SIMO system with  $M = 1$  and  $L_c = 1$ . The narrowband EM scheme modulates information only in the amplitude of the input using a non-negative-valued energy input constellation, transmitting  $X \in \mathbb{R}^+ \cup \{0\}$  such that  $X^2 \in \mathcal{C}$ . Thus the receiver does not utilize the phase of the output and computes a quadratic total energy statistic across all receive antennas,  $V = \frac{1}{N} \sum_{\mathcal{N}} |Y_r|^2$ . As  $N \rightarrow \infty$  with constant power the received statistic satisfies  $V \rightarrow X^2 + 1 \pm o(1/N)$  where the second term stems from the noise power  $\frac{1}{N} \sum_{\mathcal{N}} |Z_r|^2 \rightarrow 1$ . Thus, the receiver can decode by unequivocally mapping different received-energy regions over  $V$  to different inputs  $X$ .

In this section we define the EM scheme for a wideband system with any arbitrary Rayleigh fading block length constant  $L_c \geq 1$ . We consider the case of transmitting independent streams of information in  $M$  subchannels, with the power equally spread across all subchannels. In relation to our upper bounds in Section IV note that  $M$  is the number of active subchannels that may be selected as less than or equal to the number of available subchannels  $B = \Theta(N^\epsilon)$ . Our main

challenge is to characterize the joint error probability across  $M$  parallel EM transmissions when the power of each is  $\Theta(1/M)$  instead of constant. We show that even in this case,  $\forall \alpha > 0$  if  $M \leq \Theta(N^{\frac{1}{2}-\alpha})$  the error probability still vanishes as  $N \rightarrow \infty$  and EM can achieve an arbitrarily low probability of error when we select a constellation  $\mathcal{C}$  of a specific type such that the rate is  $M \log_2 |\mathcal{C}| = \Theta(M \log(N))$ .

To design the wideband EM achievable scheme we assume the transmitter wishes to transmit a total rate of  $R$  bits per coherence block (can be converted to  $R \frac{B_s}{L_c}$  bits per second where  $B_s$  and  $L_c$  are constants). In each band, the transmitter uses the same constellation  $\mathcal{C}$  and only one point in the energy constellation is transmitted during the  $L_c$  symbols of duration of the fading block. Hence, to transmit a total of  $R$  bits the constellation size should satisfy  $|\mathcal{C}| = 2^{R/M}$ , and to satisfy the power constraint the average power of the constellation is  $\frac{P}{M}$ . Without loss of generality let us normalize the transmitted power  $P = 1$ .

We design the wideband EM scheme for arbitrary  $L_c$  assuming an energy detector that removes the need to perform encoding across multiple symbols of the same block ( $\ell$ ). The transmitter sends  $X_{m,\ell} = \frac{\sqrt{A_m}}{\sqrt{L_c}}$  where  $A_m \in \mathcal{C}$ . In terms of the optimal capacity-achieving input distribution in Lemma 2,  $X_{\ell,m} = \sqrt{A_m} U_{m,\mathcal{L}}$ , the EM scheme replaces the IDUV  $U_{m,\mathcal{L}}$  by the all-ones normalized vector  $\frac{1}{\sqrt{L_c}}$ . Since we showed in Lemma 4 that when  $L_c$  is a constant “most of the rate” depends on the information carried by the distribution of energy, the EM scheme pays only a constant rate penalty for not using the optimal  $U_{m,\mathcal{L}}$ , and the achievable rate with this scheme achieves the scaling exponent of the capacity upper bound.

In the wideband EM scheme the receiver computes the average energy quadratic statistic in each subband  $m$  as follows:

$$V_m = \frac{1}{NL_c} \sum_{r=0}^{N-1} \left| \sum_{\ell=0}^{L_c-1} Y_{r,m,\ell} \right|^2. \quad (17)$$

Based on its knowledge of the statistics of the channel and of  $\mathcal{C}$ , the receiver divides the positive real line into non-intersecting intervals or *decoding regions*  $\{\mathcal{V}_k\}_{k=1}^{|\mathcal{C}|}$  and returns  $\hat{k} \in \{\tilde{k} : V_m \in \mathcal{V}_k\}$ .

**Theorem 2.** *In a non-coherent block fading i.i.d. Rayleigh wideband SIMO channel with  $N$  receive antennas, using equal power and rate allocation over  $M = \Theta(N^\epsilon)$  subchannels with a finite coherence time  $L_c$ , for any  $\epsilon < \frac{1}{2}$ , EM achieves a vanishing probability of error with increasing  $N$  using a constellation with transmitted rate that scales as  $R = \Theta(N^\epsilon \log(N))$ .*

*Proof.* We assume the transmitter chooses the constellation  $\mathcal{C}$  as

$$\mathcal{C} = \{0, 2d, 4d, \dots, \frac{2}{M}\}, \quad (18)$$

where we choose the half-distance between symbols as

$$d = \frac{1}{M(|\mathcal{C}|-1)} = \frac{1}{M\left(\frac{2}{M}-1\right)}, \quad (19)$$

where  $R$  is the transmission rate. We denote the scaling of this distance as  $d = \Theta\left(\frac{1}{N^t}\right)$  with exponent  $t$ . The transmitter may choose any  $d$  satisfying  $\epsilon < t < \frac{1}{2}$ , where the lower limit is required to achieve the specified transmission rate scaling and the upper limit is required by the error analysis below.

For this scheme, the transmitted rate  $R$  must have the scaling  $\Theta(N^\epsilon \log(N))$  as we have assumed in the theorem, but this rate must also satisfy an equality relative to the number of subchannels times the bits per symbol of the constellation:  $R = M \log_2 |\mathcal{C}|$ . Therefore  $R$  depends on  $d$  via the cardinality of the constellation  $|\mathcal{C}| = \Theta(N^{t-\epsilon})$ . We can show both requirements of  $R$  are compatible by writing the scaling of  $R = M \log_2 |\mathcal{C}|$  as follows

$$\begin{aligned} R &= \Theta(N^\epsilon \log_2(1 + N^{t-\epsilon})) \\ &= \Theta(N^\epsilon \log_2(N)) \end{aligned} \quad (20)$$

which agrees with the assumption of the theorem and shows that the chosen exponent  $t \geq \epsilon$  affects the rate as a multiplying constant without changing its scaling with  $N$ . We next show that we can achieve a vanishing error probability as long as we choose  $t < \frac{1}{2}$ , i.e. when the chosen separation between nearest constellation points  $d = \Theta(N^{-t})$  decays slower than  $\Theta(N^{-\frac{1}{2}})$ .

Since  $V_m$  approaches  $1 + A_m$  the centers of the decoding regions are a shifted version of the energy constellation symbols (shifted by the noise power), defined as  $\mathcal{V}_1 = (-\infty, 1 + d]$ ,  $\mathcal{V}_k = ((2k-1)d + 1, (2k+1)d + 1]$  for  $2 \leq k \leq |\mathcal{C}|-1$ , and  $\mathcal{V}_{|\mathcal{C}|} = ((2|\mathcal{C}|-1)d + 1, \infty)$ .

For these decoding regions, we consider the union bound on the probability of error over all the subchannels as follows

$$\begin{aligned} P_{\text{error}} &\leq \sum_{m=1}^M \sum_{k \in \mathcal{C}} P_{\text{error},m}(\hat{k} \neq k) \\ &\stackrel{(a)}{\approx} N^\epsilon N^{t-\epsilon} e^{-N(\min_k I_k(d))} \\ &\stackrel{(b)}{\approx} N^t e^{-N^{1-2t}}, \end{aligned} \quad (21)$$

where  $P_{\text{error},m}$  is the probability of error due to transmission in the  $m^{\text{th}}$  subband, and (a) and (b) follow from the narrowband EM analysis in [31]. Particularly, step (a) in (21) upper bounds  $P_{\text{error},m}$  using the error exponent function defined as

$$I_k(d) \triangleq \lim_{N \rightarrow \infty} \frac{-\log(\text{Prob}(|V_m - 2(k-1)d - 1| > d))}{N}. \quad (22)$$

In EM the Maximum Likelihood detector becomes the energy-based detector for the quadratic statistic  $V_m$  [31, Lemma 1]. Finally step (b) in (21) follows from the limit

$$\lim_{d \rightarrow 0} \frac{I_k(d)}{d^2} = \Theta(1) \quad (23)$$

for all  $k$ , which is proven in [31, Lemma 3].

Therefore, for  $\epsilon < \frac{1}{2}$  the transmitter can choose from a family of constellations satisfying  $\epsilon < t < \frac{1}{2}$  such that the rate is  $\Theta(N^\epsilon \log(N))$  and the right hand side expression in (21) goes to zero as  $N$  grows, completing the proof of Theorem 2.  $\square$

**Remark 4.** Note that the proof of Theorem 2 offers a collection of achievable schemes that spans a family of constellations characterized by the parameter  $t$  with  $\epsilon < t < \frac{1}{2}$ . Any constellation in this family achieves the specified rate scaling with vanishing error probability. Different constellations with different parameters  $t$  are differentiated by a trade-off between their rate and error slope, in the sense that a greater  $t$  does not modify rate scaling but increases a non-scaling constant multiplier of the achieved rate. Moreover a larger parameter  $t$  decreases the exponent that characterizes the decay speed of the error probability as  $N$  grows. Finally, the closer  $\epsilon$  is to  $\frac{1}{2}$  the narrower the range of valid constellations and for  $\epsilon = \frac{1}{2}$  the error probability union bound becomes a constant and does not vanish.

## VI. NUMERIC EXAMPLES, DISCUSSION AND EXTENSIONS

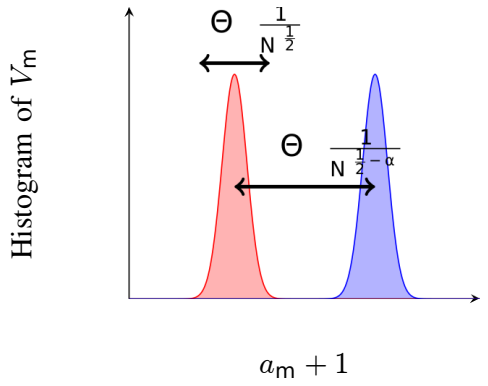
### A. Intuition behind capacity scaling

Fig. 2 provides an intuitive interpretation of Theorems 1 and 2. The values of the output energy statistic conditioned on the input energy  $p(V_m | A_m = a_m)$  are distributed around  $a_m + 1$  with most of the probability measure concentrated in a region of size  $1/N^{\frac{1}{2}}$  around the center. In Fig. 2(a) the inputs are separated as  $|a'_m - a_m| = \frac{1}{N^{\frac{1}{2}-\alpha}}$ , for  $a'_m, a_m \in \mathcal{C} : a'_m \neq a_m$ , the centers become closer at a slower pace than the tails shrink, and the transmitted symbols become easier to distinguish as  $N$  increases (Theorem 2). Conversely, in Fig. 2(b) we have  $|a'_m - a_m| = \frac{1}{N^{\frac{1}{2}+\alpha}}$ , and, as  $N$  grows, the centers of the two conditional output distributions become closer faster than their tails vanish, which is consistent with the interpretation of the proof of Lemma 3 discussed in Section IV-C.

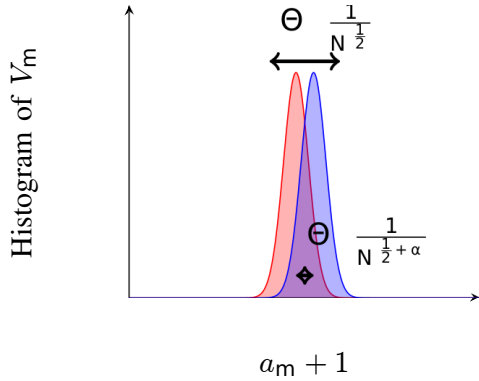
### B. Performance obtained with achievable scheme

In Figure 3 we illustrate the Bit Error Rate (BER) and the rate for a series of EM numerical simulation examples. All simulated points in the figure are obtained by the Monte-Carlo method with  $10^5$  bits per point. As a rule of thumb this number of Monte-Carlo simulations is sufficient to estimate BERs up to  $10^{-4}$ , however to conduct simulations both  $B$  and  $N$  must be integers, so we rounded the number of subchannels as  $M = \lceil N^\epsilon \rceil$ . We remark that the curves are not smooth due to the bumpy behavior of the ceiling function and not due to a lack of sufficient bits in simulation.

In Figure 3(a) we observe that the BER vanishes as  $N$  grows for schemes with  $\epsilon < \frac{1}{2}$ , whereas the error does not decay when  $\epsilon > \frac{1}{2}$ . Moreover, the error vanishes more slowly when  $\epsilon$  is close to the threshold, as expected, by the bounds in the proof of Theorem 2. In Figure 3(b) we see the transmitted rate of the EM scheme for each scenario, which is simply computed as  $M \log_2 |\mathcal{C}|$ . The rates for all EM schemes grow consistently with  $M = \lceil N^\epsilon \rceil$ , yet the rates with exponents greater than  $\frac{1}{2}$  cannot be sustained with an arbitrarily low error probability for large enough  $N$ . Here the rates are given in units of bits per channel coherence block, so for example if  $L_c/B_s = 1$  ms then the unit is Kb/s.



(a) Bandwidth-limited regime: Increasing bandwidth helps increase capacity

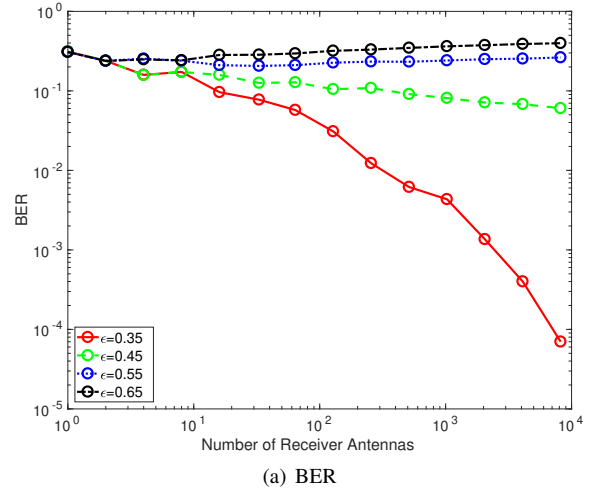


(b) Excessive bandwidth regime: Power is spread over an excessively large bandwidth

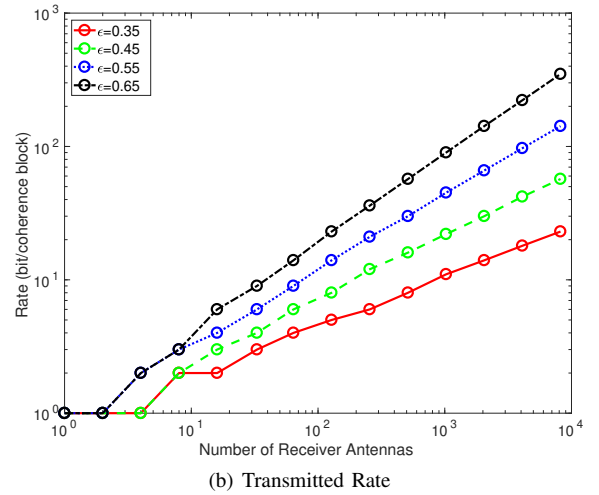
Fig. 2: Bandwidth-limited and excessive bandwidth capacity regimes

### C. Numerical plots of achievable rate with bandwidth

Figure 4 shows a numerical comparison between the capacities obtained with the genie aided coherent receiver and the pilot-assisted coherent receiver, as a fixed transmit power is spread across more and more subchannels. For the genie-aided receiver, we assume that the subchannel gains at all antennas are known precisely and the capacity is (8). For the pilot-assisted receiver we perform MMSE channel estimation using a known pilot symbol sequence with power equal to the average transmit power per subchannel for 20% of the available symbol times (i.e., the pilot overhead is 20%); and use the remaining time slots for data transmission. For calculating the rates achievable by the pilot-assisted scheme with nearest-neighbor symbol decisions, we use the spectral efficiency analysis for block-fading channels developed in [8], based on an effective SNR [8, equation (47)] that takes into account the channel estimation MMSE [8, equation (48)]. We modify our capacity expression (8) to incorporate this effective SNR rather than the actual SNR, producing  $R_{pilot-assisted} = \mathbb{E} \left[ BB_s \log \left( 1 + \frac{P(\sum_{r=0}^{N-1} |H_{r,m}|^2) (1-MMSE)}{1 + \frac{P(\sum_{r=0}^{N-1} |H_{r,m}|^2)}{B} MMSE} \right) \right]$ . We remark that nearest-neighbor symbol-by-symbol decisions are suboptimal under our channel model with pilot-assisted channel estimation, but often employed in practical devices [8]. This rate calculation method illustrates that our scaling law result



(a) BER



(b) Transmitted Rate

Fig. 3: Simulated EM channel for different values of  $\epsilon$ . Recall that  $\epsilon$  captures the relative growth of available bandwidth ( $B$ ) with the number of receiver antennas ( $N$ ), i.e.,  $B = \Theta((N)^\epsilon)$ .

is applicable not just in asymptotically large regimes of bandwidth and numbers of antennas, but also in practical systems.

We choose a sub-6 GHz band with a total available bandwidth of 100 MHz. We keep the coherence time fixed at 200 symbol times, with the subchannel bandwidth (equal to the coherence bandwidth) being 1 MHz. This corresponds to a delay spread of (on the order of) 100 ns, which is typical for small outdoor deployments. Generally, both  $B$  and  $N$  can reach several hundreds in current standards. The 3GPP New Radio specification has up to 100 MHz bandwidth [34] in the sub-6 GHz bands (more if we consider carrier aggregation). Arrays with dozens to hundreds of antennas are practical in sub-6 GHz frequencies use; for example [24] shows a 3.7GHz platform with 160 cross-polarized antennas.

The total noise power per subchannel is fixed, and the transmit power is fixed such that if there is only 1 active subchannel, the received SNR per subchannel per antenna is 3 dB. In Fig. 4 we consider a 16-antenna, a 64-antenna and a 256-antenna system.

From the figure, we observe that, while the genie-aided

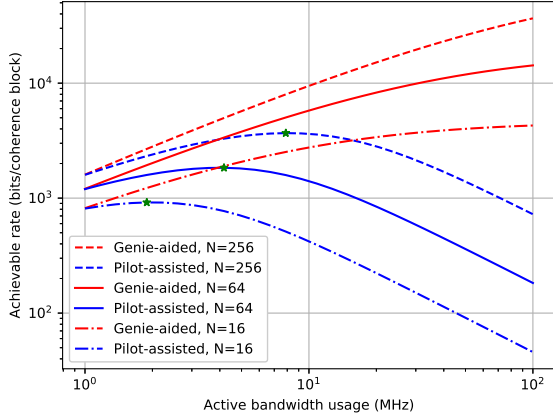


Fig. 4: Capacity comparison between genie-aided and pilot-assisted coherent schemes.  $N$  is the number of receiver antennas.

schemes are able to exploit all available spectrum for capacity improvement, the pilot assisted schemes are able to exploit only up to a certain bandwidth or, equivalently, a certain number of subchannels. If the transmit power is spread over more than the threshold number of subchannels, the channel estimation error dominates and drives down the achievable rate.

Furthermore, we represent with green stars in Fig. 4 the threshold bandwidth for the pilot-assisted receivers, that is, the maximum capacity values of the curves. The thresholds are located at 1.88, 4.17 and 7.88 MHz for 16, 64 and 256 antennas, respectively. Thus for each increase in the number of antennas by a factor of four, we see that the threshold bandwidth increases roughly by a factor of two. This is consistent with our analytical derivations concerning the joint capacity scaling behavior with a large number of antennas and a large bandwidth, which reveals that for noncoherent receivers (of which the pilot-assisted coherent receiver is a special case), there is a threshold bandwidth proportional to the square root of the number of antennas and any bandwidth in excess of this threshold does not help in enhancing the capacity scaling.

#### D. Subchannel bandwidth and coherence bandwidth

The gain associated with the frequency selective wideband channel has been modeled to be piecewise constant (and i.i.d. Rayleigh fading), with the gain being constant over the subchannel bandwidth  $B_s$ . Hence the subchannel bandwidth  $B_s$  is equal to the coherence bandwidth associated with the channel [2]. The coherence bandwidth is a property of the propagation environment, which is usually related to the inverse of the delay spread.

One possible practical interpretation of our system model is an OFDM system where the subcarrier separation is exactly  $B_s$  and the channel remains constant for  $L_c$  OFDM symbols. In many OFDM systems however, the OFDM subcarrier separation (inverse of the OFDM symbol time) is much smaller than the coherence bandwidth to ensure flatness of subcarrier gains [2]. On the other hand, our channel model is fully

general and the coherence bandwidth is a property of the block-fading channel whereas the OFDM subcarrier separation is only a property of one particular waveform. Under a careful interpretation of  $B_s$  and  $L_c$ , the non-coherent capacity bounds in our analysis hold for any waveform that can be converted into our channel model using standard transformations [18]. This includes certain cases of time-domain signaling, OFDM, SC-FDMA, or CDMA.

We defer to future work the analysis of channels where the adjacent subchannel gains are not i.i.d. and multipath channels that do not exhibit rich scattering - such as those in the mmWave bands.

#### E. Overspreading in more general channel models

We note that overspreading also appears in channel models that do not experience rich scattering. In particular, for a fixed number of antennas, Telatar and Tse showed that even sparse multipath channels experience overspreading when the delays of the paths are not known [10]. Raghavan *et al* found similar results for capacity scaling with bandwidth under sparse multipath channels [35]. Ferrante *et al* revised this framework to account for mmWave systems with Ricean fading, blockage and oxygen absorption [17].

These works suggest that our results might be applicable to a broader class of channel models than the i.i.d. Rayleigh block-fading model analyzed in this work.

#### F. Extension to MIMO and Multi-user Channels

The following remarks briefly discuss how the main observations in this paper for the single-user SIMO channel can be applicable to a MIMO single user channel and to the uplink of cellular systems where multiple single-antenna users transmit to a multi-antenna BS forming a SIMO multiple-access channel (MAC).

**Remark 5.** Consider a massive MIMO channel with the number of transmit antennas  $T$  that scales with  $N$ . Let us denote the transmit antenna index by  $t \in \mathcal{T} \triangleq \{1 \dots T\}$  and the exponent  $T = \Theta(N^\gamma)$ . A channel model generalizing (1) can be written as follows

$$Y_{r,m,\ell} = \sum_{t=1}^T H_{r,m,t} X_{m,\ell,t} + Z_{r,m,\ell}. \quad (24)$$

with non-coherent capacity  $C_n(N, B, T) \triangleq \sup_{p(X_{B,\mathcal{L},\mathcal{T}})} I(X_{B,\mathcal{L},\mathcal{T}}; Y_{N,B,\mathcal{L}})$ . It is shown in [3] that the mutual information does not increase when  $T > L_c$ , where  $L_c$  is the constant coherence block length of the fading channel. Therefore  $C_n(N, B, T) \leq C_n(N, B, \min(L_c, T))$ . Applying the chain rule we can write the upper bound  $C_n(N, B, T) \leq \min(T, L_c) C_n(N, B) = \Theta(N^{\min(\epsilon, \frac{1}{2})})$ , and the lower bound  $C_n(N, B, T) \geq C_n(N, B)$ . Therefore, when  $L_c$  is constant,  $T > 1$  can increase capacity at most by a constant but the exponent  $\gamma$  does not affect the capacity scaling.

**Remark 6.** Let us assume a multi-user SIMO channel with  $U$  users. From the classic analysis of the MAC channel

[36] we have that for any set  $\mathcal{U} \subset \{1 \dots U\}$ , the achieved rate of all the users  $u \in \mathcal{U}$ , denoted as  $R_u$ , must satisfy the sum-rate constraint  $\sum_{\mathcal{U}} R_u \leq \mathbf{I}(X_{\mathcal{B},\mathcal{L},\mathcal{U}}; Y_{\mathcal{N},\mathcal{B},\mathcal{L}})$  where  $\mathbf{I}(X_{\mathcal{B},\mathcal{L},\mathcal{U}}; Y_{\mathcal{N},\mathcal{B},\mathcal{L}})$  is the mutual information of a virtual MIMO channel formed by substituting  $\mathcal{T} = \mathcal{U}$  in (24). Therefore, the main observations of our analysis remain applicable to these constraints which, combined, enclose the capacity region of the multi-user SIMO MAC channel.

## VII. CONCLUSIONS AND FUTURE WORK

We have derived the capacity scaling laws governing the relation between large bandwidth and number of receiver antennas in coherent and non-coherent i.i.d. Rayleigh block-fading SIMO channels. We have found that in a block-fading channel of a fixed coherence length, the non-coherent capacity scales with the minimum of the number of independent subchannels and the square root of the number of receive antennas. On the other hand, coherent capacity under perfect genie-aided channel state information scales linearly with the bandwidth. We have also shown that the capacity scaling of the non-coherent channel with a large bandwidth and large number of antennas can be achieved by an energy modulation scheme with a non-coherent receiver.

Our results shed light on the inherent difficulty of supporting uplink wideband communications using a large antenna array at the receiver under a transmit power constraint. Our capacity scaling law characterizations reveal that if the number of antennas is large, and the channel realizations are not known apriori, using excessive bandwidth can actually degrade the achievable rates. This is fundamentally due to the fact that with a larger bandwidth, and hence, a larger number of subchannels, there is less power available for pilot-assisted channel estimation at each subchannel. This is in sharp contrast to what might be expected from a coherent capacity analysis with genie-aided perfect channel state information.

We finally point out that our results have focused on the scaling laws of capacities in the joint asymptotic regime of large bandwidth and large number of antennas. The capacity and capacity-achieving strategy of non-coherent systems with a finite number of antennas and bandwidth is unknown, and hence this work does not answer questions about the capacity

difference between coherent and noncoherent systems in this regime. Characterizing various properties of the non-coherent channel capacity and the capacity achieving transmission strategy remains an interesting topic for future work.

## APPENDIX A

### MUTUAL INFORMATION UPPER BOUND FOR $L_c = 1$

In this appendix we prove Lemma 3. Lemma 2 tells us that the optimal input satisfies  $X_{m,\mathcal{L}} = \sqrt{\bar{A}_m} U_{m,\mathcal{L}}$  where  $\bar{A}_m \geq 0$  and  $U_{m,\mathcal{L}}$  is a unitary isotropic vector of length  $L_c$ . For convenience we define a normalized amplitude distribution as  $\bar{A}_m \triangleq (\sum_{\ell \in \mathcal{L}} |X_{m,\ell}|^2) N^{\alpha+\frac{1}{2}} = A_m N^{\alpha+\frac{1}{2}}$ , so that we have  $\mathbb{E}[\bar{A}_0] = \Theta(1)$ .

Since  $L_c = 1$  the set  $\mathcal{L} = \{0 \dots L_c - 1\}$  becomes just the first element,  $\{0\}$ . Therefore, we replace the subindex  $\mathcal{L}$  by 0 in all symbols hereafter. For example,  $U_{m,0}$  is a unitary isotropic vector of length 1, which boils down to a uniform random phase rotation.  $\bar{A}_m$  simplifies as  $|X_{m,0}|^2 N^{\alpha+\frac{1}{2}} = A_m N^{\alpha+\frac{1}{2}}$ , and so on.

We want to upper bound the subchannel capacity function (11) with  $\mathcal{L} = \{0\}$  and the power allocation argument  $\rho_m = \frac{P}{N^{\frac{1}{2}+\alpha}}$ , which produces

$$f_C\left(\frac{P}{N^{\frac{1}{2}+\alpha}}\right) \triangleq \max_{p(X_{0,0}): \mathbb{E}[|X_{0,0}|^2] \leq \frac{P}{N^{\frac{1}{2}+\alpha}}} \mathbf{I}(X_{0,0}; Y_{\mathcal{N},0,0}). \quad (25)$$

Here without loss of generality we have chosen the subchannel index  $m = 0$  to evaluate the mutual information, which takes the same value in all the ‘‘active’’  $M = N^{\frac{1}{2}+\alpha} \leq B$  subchannels.

For any  $\xi < \alpha$ , we define the sets  $\mathcal{S}_k = [(k-1)N^{\alpha-\xi}, kN^{\alpha-\xi})$  for  $k$  belonging to the set of natural numbers  $k \in \mathbb{N}$ . We can verify that  $\cup_{k \in \mathbb{N}} \mathcal{S}_k$  covers the positive real line. We upper bound the mutual information using the sets  $\mathcal{S}_k$  and  $\bar{A}_0$  and the ‘‘indicator function’’ defined as

$$\mathbf{I}_{\bar{A}_0 \in \mathcal{S}_k} = \begin{cases} 1 & a_0 \in \mathcal{S}_k \\ 0 & a_0 \notin \mathcal{S}_k, \end{cases} \quad (26)$$

which leads to the upper bound on the mutual information integral given in (27).

$$\begin{aligned} \mathbf{I}(X_{0,0}; Y_{\mathcal{N},0,0}) &= \mathbf{I}\left(\sqrt{\bar{A}_0} N^{\alpha+\frac{1}{2}} U_{m,\mathcal{L}}; Y_{\mathcal{N},0,0}\right) \\ &= \mathbb{E}_{\bar{A}_0} \left[ \mathbb{E}_{Y_{\mathcal{N},0,0} | \bar{A}_0} \left[ \log \left( \frac{p(Y_{\mathcal{N},0,0} | \bar{A}_0)}{p(Y_{\mathcal{N},0,0})} \right) \right] \right] \\ &= \sum_{k \in \mathbb{N}} \mathbb{E}_{\bar{A}_0} \left[ \mathbb{E}_{Y_{\mathcal{N},0,0} | \bar{A}_0} \left[ \log \left( \frac{p(Y_{\mathcal{N},0,0} | \bar{A}_0)}{p(Y_{\mathcal{N},0,0})} \right) \right] \right] \\ &\stackrel{(a)}{\leq} \sum_{k \in \mathbb{N}} \mathbb{E}_{\bar{A}_0} \left[ \mathbf{I}_{\bar{A}_0 \in \mathcal{S}_k} \mathbb{E}_{Y_{\mathcal{N},0,0} | \bar{A}_0} \left[ \log \left( \frac{p(Y_{\mathcal{N},0,0} | \bar{A}_0)}{\int_{s \in \mathcal{S}_k} p(Y_{\mathcal{N},0,0} | \bar{A}_0 = s) \mu_{\bar{A}_0}(ds)} \right) \right] \right] \\ &= - \sum_{k \in \mathbb{N}} \mathbb{E}_{\bar{A}_0} \left[ \mathbf{I}_{\bar{A}_0 \in \mathcal{S}_k} \mathbb{E}_{Y_{\mathcal{N},0,0} | \bar{A}_0} \left[ \log \left( \int_{s \in \mathcal{I}_k} \frac{p(Y_{\mathcal{N},0,0} | \bar{A}_0 = s)}{p(Y_{\mathcal{N},0,0} | \bar{A}_0)} \mu_{\bar{A}_0}(ds) \right) \right] \right]. \end{aligned} \quad (27)$$

The inequality (a) follows from the fact that  $p(Y_{\mathcal{N},0,0}) \leq \int_{s \in \mathcal{S}_k} p(Y_{\mathcal{N},0,0} | \bar{A}_0 = s) \mu_{\bar{A}_0}(ds)$ , where  $\mu_X(\mathcal{A})$  refers to the measure of set  $\mathcal{A}$  under the distribution induced by the random variable  $X$ . And the last step uses the negative of the logarithm so that we can introduce the term  $p(Y_{\mathcal{N},0,0} | \bar{A}_0)$  inside the integral over  $ds$ .

Say we denote the integration variable for the average  $\mathbb{E}_{\bar{A}_0}[\cdot]$  in the above expression with the letter  $a$ . This step has allowed us to write the upper bound of the mutual information as an integral containing  $\frac{p(Y_{\mathcal{N},0,0} | \bar{A}_0 = s)}{p(Y_{\mathcal{N},0,0} | \bar{A}_0 = a)}$  where  $a$  and  $s$  are treated as independent realizations of the random variable  $\bar{A}_0$  at two different integrals.

We now show that in the limit  $N \rightarrow \infty$  the conditional distributions  $p(Y_{\mathcal{N},0,0} | \bar{A}_0 = s)$  and  $p(Y_{\mathcal{N},0,0} | \bar{A}_0 = a)$  are similar for all  $a, s \in \mathcal{S}_k$ . In particular we expand the ratio as follows

$$\frac{p(Y_{\mathcal{N},0,0} | \bar{A}_0 = s)}{p(Y_{\mathcal{N},0,0} | \bar{A}_0 = a)} = \left( \frac{1 + \frac{a}{N^{\frac{1}{2} + \alpha}}}{1 + \frac{s}{N^{\frac{1}{2} + \alpha}}} \right)^N \times e^{-(\sum_{r=0}^{N-1} |Y_{r,0,0}|^2)} \left( \frac{1 + \frac{s}{N^{\frac{1}{2} + \alpha}}}{1 + \frac{a}{N^{\frac{1}{2} + \alpha}}} \right). \quad (28)$$

Defining the difference  $\Delta a = s - a$ , this may be written as

$$\frac{p(Y_{\mathcal{N},0,0} | \bar{A}_0 = s)}{p(Y_{\mathcal{N},0,0} | \bar{A}_0 = a)} = \left( 1 + \frac{\frac{\Delta a}{N^{\frac{1}{2} + \alpha}}}{1 + \frac{a}{N^{\frac{1}{2} + \alpha}}} \right)^{-N} \times e^{-NG \left( \frac{-\frac{\Delta a}{N^{\frac{1}{2} + \alpha}}}{\left(1 + \frac{a}{N^{\frac{1}{2} + \alpha}}\right) \left(1 + \frac{a}{N^{\frac{1}{2} + \alpha}} + \frac{\Delta a}{N^{\frac{1}{2} + \alpha}}\right)} \right)} \doteq e^{-N \frac{\Delta a}{N^{\frac{1}{2} + \alpha}} (1-G)}. \quad (29)$$

where  $G \triangleq \frac{\sum_{r=0}^{N-1} |Y_{r,0,0}|^2}{N}$ , and we use the result that  $(1 +$

$f(N))^{t(N)} \doteq e^{f(N)t(N)}$  if  $f(N) \rightarrow 0, t(N) \rightarrow \infty$ , such that  $f(N)t(N) \rightarrow \infty$ . We now observe that, as  $N \rightarrow \infty$ , by the central limit theorem,  $\sqrt{N}(G - 1 - \frac{a}{N^{\frac{1}{2} + \alpha}})$  converges to a zero mean normal random variable independent of  $a$  with a variance independent of  $N$ .

We can now use (29) to write the part inside the logarithm as follows

$$\int_{s \in \mathcal{S}_k} \frac{1}{p_k} \frac{p(Y_{\mathcal{N},0,0} | \bar{A}_0 = s)}{p(Y_{\mathcal{N},0,0} | \bar{A}_0 = a)} \mu_{\bar{A}_0}(ds) = \int_{s \in \mathcal{I}_k} \frac{1}{p_k} e^{-T(s,G,\bar{A}_0)} \mu_{\bar{A}_0}(ds) = 1 - \Theta \left( \int_{s \in \mathcal{S}_k} \frac{p(s)}{p_k} T(s,G,a) ds \right), \quad (30)$$

where  $T(s,G,a) = \left( N \frac{(s-a)}{N^{\frac{1}{2} + \alpha}} (1-G) \right)$ . The last step follows from the CLT and the observation that

$$\lim_{N \rightarrow \infty} T(s,G,a) = \lim_{N \rightarrow \infty} N \frac{s-a}{N^{\frac{1}{2} + \alpha}} \frac{a}{N^{\frac{1}{2} + \alpha}} = 0. \quad (31)$$

Writing down all the steps in the integral  $\mathbb{E}_{\bar{A}_0}[\cdot]$  with variable  $a \in \mathcal{S}_k$  we get (32), where (a) is (27) and (b) comes from (28),(29),(30). In (c) we use  $\log(1-x) = -\Theta(x)$  as  $x \rightarrow 0$ . In (d) we use the average of  $G$  according to CLT, and (e) is just cleanup.

Using  $\int \mu_{\bar{A}_0}(ds) = 1, (\int a \mu_{\bar{A}_0}(da)) (\int s \mu_{\bar{A}_0}(ds)) = \Theta(1)$ , and  $|s-a| < \Theta(N^{\alpha-\xi})$ , due to the assumption that  $a, s \in \mathcal{S}_k$ , we get that,

$$\mathbb{E}_{\bar{A}_0} \left[ \mathbb{E}_{Y_{\mathcal{N},0,0} | \bar{A}_0} \left[ \log \left( \frac{p(Y_{\mathcal{N},0,0} | \bar{A}_0)}{p(Y_{\mathcal{N},0,0})} \right) \right] \right] \leq \Theta(N^{-\alpha-\xi}). \quad (33)$$

Since this must be satisfied for any  $\xi \leq \alpha$  the tightest bound is choosing  $\xi = \alpha$  producing

$$\begin{aligned} I(X_{0,0}; Y_{\mathcal{N},0,0}) &= \mathbb{E}_{\bar{A}_0} \left[ \mathbb{E}_{Y_{\mathcal{N},0,0} | \bar{A}_0} \left[ \log \left( \frac{p(Y_{\mathcal{N},0,0} | \bar{A}_0)}{p(Y_{\mathcal{N},0,0})} \right) \right] \right] \\ &\stackrel{(a)}{\leq} - \sum_{k=1}^{\infty} \int_{a \in \mathcal{S}_k} \mathbb{E}_{Y_{\mathcal{N},0,0} | \bar{A}_0 = a} \left[ \log \int_{s \in \mathcal{S}_k} \frac{1}{p_k} \frac{p(Y_{\mathcal{N},0,0} | \bar{A}_0 = s)}{p(Y_{\mathcal{N},0,0} | \bar{A}_0 = a)} \mu_{\bar{A}_0}(ds) \right] \mu_{\bar{A}_0}(da) \\ &\stackrel{(b)}{=} \sum_{k=1}^{\infty} - \int_{a \in \mathcal{S}_k} \mathbb{E}_{Y_{\mathcal{N},0,0} | a} \left[ \log \left( 1 - \Theta \left( \int_{s \in \mathcal{S}_k} \frac{1}{p_k} T(s,G,a) \mu_{\bar{A}_0}(ds) \right) \right) \right] \mu_{\bar{A}_0}(da) \\ &\stackrel{(c)}{\leq} \sum_{k=1}^{\infty} \int_{a \in \mathcal{S}_k} \int_{s \in \mathcal{S}_k} \Theta(N) \left( \frac{s-a}{N^{\frac{1}{2} + \alpha}} \right) (1 - \mathbb{E}_{Y_{\mathcal{N},0,0} | a} [G]) \mu_{\bar{A}_0}(ds) \mu_{\bar{A}_0}(da) \\ &\stackrel{(d)}{=} \sum_{k=1}^{\infty} \int_{a \in \mathcal{S}_k} \int_{s \in \mathcal{S}_k} N \left( \frac{s-a}{N^{\frac{1}{2} + \alpha}} \right) \left( 1 - 1 - \frac{a}{N^{\frac{1}{2} + \alpha}} \right) \mu_{\bar{A}_0}(ds) \mu_{\bar{A}_0}(da) \\ &\stackrel{(e)}{=} \sum_{k=1}^{\infty} \int_{a \in \mathcal{S}_k} \int_{s \in \mathcal{S}_k} N^{-2\alpha} ((a-s)a) \mu_{\bar{A}_0}(ds) \mu_{\bar{A}_0}(da), \end{aligned} \quad (32)$$

$$\begin{aligned} \mathbf{I}(X_{0,0}; Y_{\mathcal{N},0,0}) &= \mathbb{E}_{\bar{A}_0} \left[ \mathbb{E}_{Y_{\mathcal{N},0,0}|\bar{A}_0} \left[ \log \left( \frac{p(Y_{\mathcal{N},0,0}|\bar{A}_0)}{p(Y_{\mathcal{N},0,0})} \right) \right] \right] \\ &\leq \Theta(N^{-2\alpha}). \end{aligned} \quad (34)$$

## APPENDIX B

### MUTUAL INFORMATION UPPER BOUND FOR $L_c \geq 1$

Lemma 2 specifies that the optimal input satisfies  $X_{m,\mathcal{L}} = \sqrt{A_m} U_{m,\mathcal{L}}$  where  $A_m > 0$  and  $U_{m,\mathcal{L}}$  is a unitary isotropic vector of length  $L_c$ . It is known that

$$\sum_{\ell \in \mathcal{L}} |U_{m,\ell}|^2 = 1. \quad (35)$$

We next write down the distribution of the output for subchannel  $m = 0$ , denoted  $Y_{\mathcal{N},0,\mathcal{L}}$ , given a fixed input  $X_{0,\mathcal{L}}$ . We have

$$\begin{aligned} p(Y_{\mathcal{N},0,\mathcal{L}}|X_{0,\mathcal{L}}) &= \frac{\int e^{-\sum_{r=0}^{N-1} \sum_{\ell=0}^{L_c-1} |Y_{r,0,\ell} - H_{r,0} X_{0,\ell}|^2} e^{-\sum_{r=0}^{N-1} |H_{r,0}|^2} dH_{\mathcal{N}}}{\pi^{NL_c}} \\ &= \frac{\int e^{-\sum_{r=0}^{N-1} \sum_{\ell=0}^{L_c-1} |Y_{r,0,\ell} - H_{r,0} \sqrt{A_0} U_{0,\ell}|^2} e^{-\sum_{r=0}^{N-1} |H_{r,0}|^2} dH_{\mathcal{N}}}{\pi^{NL_c}} \\ &= \frac{e^{(-\sum_{r=0}^{N-1} \sum_{\ell=0}^{L_c-1} |Y_{r,0,\ell}|^2) + \sum_{r=0}^{N-1} \frac{|\sum_{\ell=0}^{L_c-1} Y_{r,0,\ell} \sqrt{A_0} v_{0,\ell}^*|^2}{1+A_0}}}{\pi^{NL_c} (1+A_0)^N} \end{aligned} \quad (36)$$

Similar to the proof for  $L_c = 1$ , we now proceed to define a normalized amplitude distribution as  $\bar{A}_0 \triangleq (\sum_{\ell \in \mathcal{L}} |X_{0,\ell}|^2) N^{\alpha+\frac{1}{2}} = A_0 N^{\alpha+\frac{1}{2}}$ . Observe that

$$\mathbb{E}[\bar{A}_0] = L_c = \Theta(1). \quad (37)$$

We now proceed to find the ratio of two conditional distributions for two different realizations of  $X_{0,\mathcal{L}}$ . As in the case  $L_c = 1$ , such a ratio will be found inside an average where  $a$  and  $b$  (respectively  $u_{0,\mathcal{L}}$  and  $v_{0,\mathcal{L}}$ ) will be integration variables treated as independent realizations of the variable  $\bar{A}_0$  (respectively  $U_{0,\mathcal{L}}$ ) for integration purposes. We have:

$$\begin{aligned} \frac{p(Y_{\mathcal{N},0,\mathcal{L}}|\bar{A}_0 = a, U_{0,\mathcal{L}} = u_{0,\mathcal{L}})}{p(Y_{\mathcal{N},0,\mathcal{L}}|\bar{A}_0 = b, U_{0,\mathcal{L}} = v_{0,\mathcal{L}})} &= \frac{e^{\sum_{r=0}^{N-1} \frac{|\sum_{\ell=0}^{L_c-1} Y_{r,0,\ell} \sqrt{\frac{a}{N^{\frac{1}{2}+\alpha}}} u_{0,\ell}^*|^2}{1+\frac{a}{N^{\frac{1}{2}+\alpha}}}}}{e^{\sum_{r=0}^{N-1} \frac{|\sum_{\ell=0}^{L_c-1} Y_{r,0,\ell} \sqrt{\frac{b}{N^{\frac{1}{2}+\alpha}}} v_{0,\ell}^*|^2}{1+\frac{b}{N^{\frac{1}{2}+\alpha}}}}} \end{aligned} \quad (38)$$

We now make an observation about the exponents. We note that, if  $a, b \in \mathcal{S}_k$  for a fixed  $k$ ,  $\frac{a}{N^{\frac{1}{2}+\alpha}}, \frac{b}{N^{\frac{1}{2}+\alpha}} \rightarrow 0$  as  $N \rightarrow \infty$ , and we thus obtain (39) where the notation  $f(N) \doteq g(N)$  represents  $\lim_{N \rightarrow \infty} f(N) - g(N) = 0$ .

We now observe the following: under the distribution  $p(Y_{\mathcal{N},0,\mathcal{L}}|\bar{A}_0 = b, U_{0,\mathcal{L}} = v_{0,\mathcal{L}})$ , we have

$$\left| \sum_{\ell=0}^{L_c-1} Y_{r,0,\ell} v_{0,\ell}^* \right| = \left| \sqrt{b \frac{|\sum_{\ell \in \mathcal{L}} u_{0,\ell}^* v_{0,\ell}|^2}{N^{\frac{1}{2}+\alpha}}} + \tilde{Z}_0 \right|, \quad (40)$$

and

$$\sum_{\ell=0}^{L_c-1} Y_{r,0,\ell} v_{0,\ell}^* = \sqrt{\frac{b}{N^{\frac{1}{2}+\alpha}}} + \hat{Z}_0, \quad (41)$$

where  $\tilde{Z}_0$  and  $\hat{Z}_0$  are zero mean complex Gaussians of unit second moment, with  $\mathbb{E}[\tilde{Z}_0 \hat{Z}_0^*] = \sum_{\ell=0}^{L_c-1} u_{0,\ell} v_{0,\ell}^* \triangleq t(u_{0,\mathcal{L}}, v_{0,\mathcal{L}})$ . By concentration of measure, we have that

$$\begin{aligned} G &\triangleq \frac{1}{N} \sum_{r=0}^{N-1} \left( \left( \frac{|\sum_{\ell=0}^{L_c-1} Y_{r,0,\ell} u_{0,\ell}^*|^2}{N^{\frac{1}{2}+\alpha}} - \left( \frac{|\sum_{\ell=0}^{L_c-1} Y_{r,0,\ell} v_{0,\ell}^*|^2}{N^{\frac{1}{2}+\alpha}} \right) \right) \right) \\ &\sim \frac{a-b}{N^{\frac{1}{2}+\alpha}} \left( 1 + \frac{m(u_{0,\mathcal{L}}, v_{0,\mathcal{L}})}{\sqrt{N}} \right) \\ &\quad + \frac{a}{N^{\frac{1}{2}+\alpha}} \frac{b}{N^{\frac{1}{2}+\alpha}} \left| \sum_{\ell \in \mathcal{L}} u_{0,\ell}^* v_{0,\ell} \right|^2 \\ &\quad - \left( \frac{b}{N^{\frac{1}{2}+\alpha}} \right)^2 + \text{lower order terms}, \end{aligned} \quad (42)$$

where  $\sim$  stands for “distributed as”,  $\nu$  (defined as  $\frac{\sqrt{N(G-1)}}{m(u_{0,\mathcal{L}}, v_{0,\mathcal{L}})}$ ) is distributed as a Gaussian random variable independent of  $u_{0,\mathcal{L}}$  and  $v_{0,\mathcal{L}}$ , and

$$m^2(u_{0,\mathcal{L}}, v_{0,\mathcal{L}}) = (a+b)^2 - 2ab \mathbb{E} \left[ |\tilde{Z}_0 \hat{Z}_0|^2 \right]. \quad (43)$$

Observe that, when  $t(u_{0,\mathcal{L}}, v_{0,\mathcal{L}}) = 1$ , i.e., when  $u_{0,\mathcal{L}} = v_{0,\mathcal{L}}$ , we have  $m^2(u_{0,\mathcal{L}}, v_{0,\mathcal{L}}) = (a-b)^2$ , and when  $t(u_{0,\mathcal{L}}, v_{0,\mathcal{L}}) = 0$ ,  $m^2(u_{0,\mathcal{L}}, v_{0,\mathcal{L}}) = a^2 + b^2$ . Thus

$$(a-b)^2 \leq m^2(u_{0,\mathcal{L}}, v_{0,\mathcal{L}}) \leq a^2 + b^2, \quad (44)$$

and the maximum variation in the value of  $m^2(u_{0,\mathcal{L}}, v_{0,\mathcal{L}})$  across all values of  $u_{0,\mathcal{L}}$  is bounded by  $\Theta(ab)$ .

We can then simplify (39) to give

$$\begin{aligned} (38) &\doteq \left( 1 + \frac{b-a}{N^{\frac{1}{2}+\alpha}} \right)^N e^{\sum_{r=0}^{N-1} \left( \left( \frac{|\sum_{\ell=0}^{L_c-1} Y_{r,0,\ell} u_{0,\ell}^*|^2}{N^{\frac{1}{2}+\alpha}} \right) \left( \frac{a}{N^{\frac{1}{2}+\alpha}} \left( 1 - \frac{a}{N^{\frac{1}{2}+\alpha}} \right) \right) - \left( \frac{|\sum_{\ell=0}^{L_c-1} Y_{r,0,\ell} v_{0,\ell}^*|^2}{N^{\frac{1}{2}+\alpha}} \right) \left( \frac{b}{N^{\frac{1}{2}+\alpha}} \left( 1 - \frac{b}{N^{\frac{1}{2}+\alpha}} \right) \right) \right)} \\ &\doteq e^{N \frac{b-a}{N^{\frac{1}{2}+\alpha}}} e^{\sum_{r=0}^{N-1} \left( \left( \frac{|\sum_{\ell=0}^{L_c-1} Y_{r,0,\ell} u_{0,\ell}^*|^2}{N^{\frac{1}{2}+\alpha}} \right) \frac{a}{N^{\frac{1}{2}+\alpha}} - \left( \frac{|\sum_{\ell=0}^{L_c-1} Y_{r,0,\ell} v_{0,\ell}^*|^2}{N^{\frac{1}{2}+\alpha}} \right) \frac{b}{N^{\frac{1}{2}+\alpha}} \right)}. \end{aligned} \quad (39)$$

## REFERENCES

- [1] M. Chowdhury, A. Manolacos, F. Gómez-Cuba, E. Erkip, and A. J. Goldsmith, "Capacity scaling in noncoherent wideband massive SIMO systems," in *IEEE Information Theory Workshop (ITW)*, 2015.
- [2] A. Goldsmith, *Wireless communications*. Cambridge University Press, 2005.
- [3] T. L. Marzetta and B. M. Hochwald, "Capacity of a mobile multiple-antenna communication link in Rayleigh flat fading," *IEEE Transactions on Information Theory*, vol. 45, no. 1, pp. 139–157, 1999.
- [4] M. Katz and S. Shamai, "On the capacity-achieving distribution of the discrete-time noncoherent and partially coherent AWGN channels," *IEEE Transactions on Information Theory*, vol. 50, no. 10, pp. 2257–2270, 2004.
- [5] R. R. Perera, T. S. Pollock, and T. D. Abhayapala, "Non-coherent Rayleigh fading MIMO channels: Capacity and optimal input," in *IEEE International Conference on Communications (ICC)*, 2006, pp. 4180–4185.
- [6] A. Lozano, "Interplay of spectral efficiency, power and Doppler spectrum for reference-signal-assisted wireless communication," *IEEE Transactions on Wireless Communications*, vol. 7, no. 12, pp. 5020–5029, 2008.
- [7] V. Sethuraman, L. Wang, B. Hajek, and A. Lapidoth, "Low-SNR capacity of noncoherent fading channels," *IEEE Transactions on Information Theory*, vol. 55, no. 4, pp. 1555–1574, 2009.
- [8] N. Jindal and A. Lozano, "A unified treatment of optimum pilot overhead in multipath fading channels," *IEEE Transactions on Communications*, vol. 58, no. 10, pp. 2939–2948, 2010.
- [9] M. Chowdhury and A. Goldsmith, "Capacity of block Rayleigh fading channels without CSI," in *2016 IEEE International Symposium on Information Theory (ISIT)*, 2016, pp. 1884–1888.
- [10] İ. E. Telatar and D. N. Tse, "Capacity and mutual information of wideband multipath fading channels," *IEEE Transactions on Information Theory*, vol. 46, no. 4, pp. 1384–1400, 2000.
- [11] M. Médard and R. G. Gallager, "Bandwidth scaling for fading multipath channels," *IEEE Transactions on Information Theory*, vol. 48, no. 4, pp. 840–852, 2002.
- [12] S. Verdú, "Spectral efficiency in the wideband regime," *IEEE Transactions on Information Theory*, vol. 48, no. 6, pp. 1319–1343, 2002.
- [13] M. Medard, "On approaching wideband capacity using multitone FSK," *IEEE Journal on Selected Areas in Communications*, vol. 23, no. 9, pp. 1830–1838, 2005.
- [14] L. Zheng, D. N. C. Tse, and M. Medard, "Channel coherence in the low-SNR regime," *IEEE Transactions on Information Theory*, vol. 53, no. 3, pp. 976–997, 2007.
- [15] S. Ray, M. Medard, and L. Zheng, "On noncoherent MIMO channels in the wideband regime: capacity and reliability," *IEEE Transactions on Information Theory*, vol. 53, no. 6, pp. 1983–2009, 2007.

$$\begin{aligned}
& \frac{p(Y_{N,0,\mathcal{L}}|\bar{A}_0 = a, U_{0,\mathcal{L}} = u_{0,\mathcal{L}})}{p(Y_{N,0,\mathcal{L}}|\bar{A}_0 = b, U_{0,\mathcal{L}} = v_{0,\mathcal{L}})} \\
& \doteq e^{\frac{(b-a)N + \sum_{r=0}^{N-1} (a(|\sum_{\ell=0}^{L_c-1} Y_{r,0,\ell} u_{0,\ell}^*|^2) - b(|\sum_{\ell=0}^{L_c-1} Y_{r,0,\ell} v_{0,\ell}^*|^2))}{N^{\frac{1}{2}+\alpha}}} \\
& \doteq e^{N\left(\frac{b-a}{N^{\frac{1}{2}+\alpha}} + G\right)} \\
& \doteq e^{N\left(\frac{a-b}{N^{\frac{1}{2}+\alpha}} \frac{m(u_{0,\mathcal{L}}, v_{0,\mathcal{L}})\nu}{\sqrt{N}} - \frac{b}{N^{\frac{1}{2}+\alpha}} \left(\frac{b-a|\sum_{\ell \in \mathcal{L}} u_{0,\ell}^* v_{0,\ell}|^2}{N^{\frac{1}{2}+\alpha}}\right)\right)}. \tag{45}
\end{aligned}$$

From Laplace's principle, we then get (46) as  $N \rightarrow \infty$ . Observe that the denominator is independent of  $v_{0,\mathcal{L}}$  in the limit as  $N \rightarrow \infty$ . We now observe that

$$\begin{aligned}
& \max_{u_{0,\mathcal{L}}} N \left( \frac{a-b}{N^{\frac{1}{2}+\alpha}} \frac{m(u_{0,\mathcal{L}}, v_{0,\mathcal{L}})\nu}{\sqrt{N}} - \frac{b}{N^{\frac{1}{2}+\alpha}} \left(\frac{b-a|\sum_{\ell \in \mathcal{L}} u_{0,\ell}^* v_{0,\ell}|^2}{N^{\frac{1}{2}+\alpha}}\right) \right) \\
& \triangleq M(a, b, \nu) \\
& = \begin{cases} N \left( \frac{a-b}{N^{\frac{1}{2}+\alpha}} \frac{|a-b|\nu}{\sqrt{N}} - \frac{b}{N^{\frac{1}{2}+\alpha}} \left(\frac{b-a}{N^{\frac{1}{2}+\alpha}}\right) \right) & \text{if } (a-b)\nu < 0, \\ N \left( \frac{a-b}{N^{\frac{1}{2}+\alpha}} + \frac{\sqrt{a^2+b^2}\nu}{\sqrt{N}} - \left(\frac{b}{N^{\frac{1}{2}+\alpha}}\right)^2 \right) & \text{if } (a-b)\nu > 0, \end{cases} \tag{47}
\end{aligned}$$

for a large enough  $N$ .

We now bound the mutual information for subchannel 0. Using the same definition of  $\mathcal{S}_k$  that we had in Appendix A, we have that the mutual information in the subchannel 0 is given by (48) where (a) follows from (47) and the observation that  $\nu$  in (47) is independent of  $U_{0,\mathcal{L}}$  in the limit. (b) follows from the fact that  $E_{\nu|b} [M(a, b, \nu)] = -\frac{b^2}{N^{2\alpha}} + \frac{1}{2} \frac{ab}{N^{2\alpha}}$ . (c) is established exactly the same way as in Appendix A. This concludes the proof.

---


$$\frac{\log\left(\int \frac{p(Y_{N,0,\mathcal{L}}|\bar{A}_0=a, U_{0,\mathcal{L}}=u_{0,\mathcal{L}})}{p(Y_{N,0,\mathcal{L}}|\bar{A}_0=b, U_{0,\mathcal{L}}=v_{0,\mathcal{L}})} \mu_{U_{0,\mathcal{L}}}(du_{0,\mathcal{L}})\right)}{\max_{u_{0,\mathcal{L}}} N \left( \frac{a-b}{N^{\frac{1}{2}+\alpha}} \frac{m(u_{0,\mathcal{L}}, v_{0,\mathcal{L}})\nu}{\sqrt{N}} - \frac{b}{N^{\frac{1}{2}+\alpha}} \left(\frac{b}{N^{\frac{1}{2}+\alpha}} - \frac{a}{N^{\frac{1}{2}+\alpha}} |\sum_{\ell \in \mathcal{L}} u_{0,\ell}^* v_{0,\ell}|^2\right) \right)} \rightarrow 1. \tag{46}$$


---

$$\begin{aligned}
I(X_{0,0}; Y_{N,0,\mathcal{L}}) &= E_{\bar{A}_0, U_{0,\mathcal{L}}} \left[ E_{Y_{N,0,\mathcal{L}}|\bar{A}_0, U_{0,\mathcal{L}}} \left[ \log \left( \frac{p(Y_{N,0,\mathcal{L}}|\bar{A}_0, U_{0,\mathcal{L}})}{p(Y_{N,0,\mathcal{L}})} \right) \right] \right] \\
&\leq \sum_{k=1}^{\infty} E_{\bar{A}_0, U_{0,\mathcal{L}}} \left[ \mathbf{I}_{\bar{A}_0 \in \mathcal{S}_k} E_{Y_{N,0,\mathcal{L}}|\bar{A}_0, U_{0,\mathcal{L}}} \left[ \log \left( \frac{p(Y_{N,0,\mathcal{L}}|\bar{A}_0, U_{0,\mathcal{L}})}{\int_{a \in \mathcal{S}_k} \int_u p(Y_{N,0,\mathcal{L}}|a, u) \mu_{U_{0,\mathcal{L}}}(du) \mu_{\bar{A}_0}(da)} \right) \right] \right] \\
&\stackrel{(a)}{=} \sum_{k=1}^{\infty} E_{\bar{A}_0, U_{0,\mathcal{L}}} \left[ \mathbf{I}_{\bar{A}_0 \in \mathcal{S}_k} E_{Y_{N,0,\mathcal{L}}|\bar{A}_0, U_{0,\mathcal{L}}} \left[ - \int_{a \in \mathcal{S}_k} M(a, \bar{A}_0, \nu) \mu_{\bar{A}_0}(da) \right] \right] \\
&\stackrel{(b)}{=} \sum_{k \in \mathbb{N}} \int_{b \in \mathcal{S}_k} \int_{a \in \mathcal{S}_k} \left( \frac{b^2}{N^{2\alpha}} - \frac{1}{2} \frac{ab}{N^{2\alpha}} \right) \mu_{\bar{A}_0}(da) \mu_{\bar{A}_0}(db) \\
&\stackrel{(c)}{=} \Theta(N^{-2\alpha}). \tag{48}
\end{aligned}$$

- [16] A. Lozano and D. Porrat, "Non-peaky signals in wideband fading channels: Achievable bit rates and optimal bandwidth." *IEEE Transactions on Wireless Communications*, vol. 11, no. 1, pp. 246–257, 2012.
- [17] G. C. Ferrante, T. Q. S. Quek, and M. Z. Win, "Revisiting the capacity of noncoherent fading channels in mmWave system," *IEEE International Conference on Communications, ICC*, vol. 65, no. 8, pp. 3259–3275, 2016.
- [18] F. Gómez-Cuba, J. Du, M. Médard, and E. Erkip, "Unified capacity limit of non-coherent wideband fading channels," *IEEE Transactions on Wireless Communications*, vol. 16, no. 1, pp. 43–57, 2017.
- [19] J. Du and R. A. Valenzuela, "How much spectrum is too much in millimeter wave wireless access," vol. 8716, no. c, pp. 1–15, 2017.
- [20] A. M. Tulino and S. Verdú, "Random matrix theory and wireless communications." *Foundations and Trends in Communications and Information Theory*, vol. 1, no. 1, 2004.
- [21] T. L. Marzetta, "How much training is required for multiuser MIMO?" in *IEEE 40th Asilomar Conference on Signals, Systems and Computers (ACSSC)*, 2006, pp. 359–363.
- [22] T. L. Marzetta, G. Caire, M. Debbah, I. Chih-Lin, and S. K. Mohammed, "Special issue on massive MIMO," *Journal of Communications and Networks*, vol. 15, no. 4, pp. 333–337, 2013.
- [23] E. Björnson, E. G. Larsson, and M. Debbah, "Massive MIMO for maximal spectral efficiency: How many users and pilots should be allocated?" *IEEE Transactions on Wireless Communications*, vol. 15, no. 2, pp. 1293–1308, 2016.
- [24] E. Björnson, E. G. Larsson, and T. L. Marzetta, "Massive MIMO: ten myths and one critical question," *IEEE Communications Magazine*, vol. 54, no. 2, pp. 114–123, 2016.
- [25] L. Zheng and D. Tse, "Optimal diversity-multiplexing trade-off in multi-antenna channels," in *Proc. of the 39th Allerton Conference on Communication, Control and Computing*, 2001, pp. 835–844.
- [26] L. Zheng and D. N. C. Tse, "Sphere packing in the Grassmann manifold: A geometric approach to the noncoherent multi-antenna channel," in *2000 IEEE International Symposium on Information Theory*, 2000, pp. 364–364.
- [27] E. Björnson, J. Hoydis, and L. Sanguinetti, "Massive MIMO has unlimited capacity," *IEEE Transactions on Wireless Communications*, vol. 17, no. 1, pp. 574–590, 2018.
- [28] A. Manolakos, M. Chowdhury, and A. J. Goldsmith, "Constellation design in noncoherent massive SIMO systems," in *IEEE Global Telecommunications Conference (GLOBECOM)*, 2014.
- [29] M. Chowdhury, A. Manolakos, and A. J. Goldsmith, "Design and performance of non coherent massive SIMO systems," in *IEEE Annual Conference on Information Sciences and Systems (CISS)*, 2014, pp. 1–6.
- [30] A. Manolakos, M. Chowdhury, and A. Goldsmith, "Energy-based modulation for noncoherent massive SIMO systems," *IEEE Transactions on Wireless Communications*, vol. 15, no. 11, pp. 7831–7846, 2016.
- [31] M. Chowdhury, A. Manolakos, and A. Goldsmith, "Scaling laws for noncoherent energy-based communications in the SIMO MAC," *IEEE Transactions on Information Theory*, vol. 62, no. 4, pp. 1980–1992, 2016.
- [32] D. E. Knuth, "Big Omicron and big Omega and big Theta," *ACM SIGACT News*, vol. 8, no. 2, pp. 18–24, 1976.
- [33] A. Lozano and N. Jindal, "Are yesterday's information-theoretic fading models and performance metrics adequate for the analysis of today's wireless systems?" *IEEE Communications Magazine*, vol. 50, no. 11, pp. 210–217, 2012.
- [34] 3GPP, "3rd Generation Partnership Project; Technical Specification Group Radio Access Network; NR; NR and NG-RAN Overall Description; Stage 2 (Release 15)," *3GPP TS 38 300*, no. Release 15, 2019.
- [35] V. Raghavan, G. Hariharan, and A. M. Sayeed, "Capacity of Sparse Multipath Channels in the Ultra-Wideband Regime," *IEEE Journal of Selected Topics in Signal Processing*, vol. 1, no. 3, pp. 357–371, 2007.
- [36] T. M. Cover and J. a. Thomas, *Elements of Information Theory*, ser. Wiley Series in Telecommunications. New York, USA: John Wiley & Sons, Inc., 1991, vol. 6.